World Academy of Science, Engineering and Technology
International Journal of Mechanical and Mechatronics Engineering
Vol:13, No:7, 2019

A Numerical Study on the Effects of N_2 Dilution on the Flame Structure and Temperature Distribution of Swirl Diffusion Flames

Yasaman Tohidi, Shidvash Vakilipour, Saeed Ebadi Tavallaee, Shahin Vakilipoor Takaloo, Hossein Amiri

Open Science Index, Mechanical and Mechatronics Engineering Vol:13, No:7, 2019 publications.waset.org/10010559/pdf

***Abstract*—**The numerical modeling is performed to study the effects of N_2 addition to the fuel stream on the flame structure and temperature distribution of methane-air swirl diffusion flames with different swirl intensities. The Open source Field Operation and Manipulation (OpenFOAM) has been utilized as the computational tool. Flamelet approach along with modified k-ε model is employed to model the flame characteristics. The results indicate that the presence of N_2 in the fuel stream leads to the flame temperature reduction. By increasing of swirl intensity, the flame structure changes significantly. The flame has a conical shape in low swirl intensity; however, it has an hour glass-shape with a shorter length in high swirl intensity. The effects of N_2 dilution decrease the flame length in all swirl intensities; however, the rate of reduction is more noticeable in low swirl intensity.

***Keywords*—**Swirl diffusion flame, N_2 dilution, OpenFOAM, Swirl intensity.

I. Introduction

THE increasing of Nitrogen Oxides (NO_x) in the atmosphere has become a major concern in recent years. Since the high level of NO_x is detrimental for human health [1], different strategies to reduce this pollutant emission has been taken into consideration by several researchers. In practical applications, the addition of N_2 and other gases like CO_2 and H_2O as a diluent to the fuel or oxidizer stream is commonly used to decrease flame temperature and achieve lower pollutant emissions [2], [3]. Diluent addition has a significant impact on the flame structure, flammability limits and pollutant emissions. Several researchers have investigated the effect of dilution on flame characteristics.

Park et al. [4] studied the effect of different diluents in methane-air counter-flow diffusion flames and showed that thermal effect of N_2 addition leads to the flame temperature reduction. Zhuo et al. [5] conducted a numerical study on the impact of N_2, CO_2, and H_2O addition on combustion characteristics of syngas turbulent non-premixed jet flames. Their results indicated that N_2 is an effective diluent for flame temperature reduction. Also, they showed that the N_2 addition shortens the flame size. Wang et al. [6] performed a numerical investigation on the physical and chemical effects of CO_2 and H_2O additives in the methane diffusion flames. They focused on the thermal and chemical effects of theses diluents on the flame temperature and Emission Index of CO (EICO). Xu et al. [7] investigated the effect of H_2O and CO_2 dilution on the structure and shape of coflow diffusion flames. They reported that the thermal and chemical effects of CO_2 replacement of N_2 in air would lead to the reduction of flame temperature. Gascoin et al. [8] considered the effect of diluent addition on the flame temperature distribution. Cho and Chung [9] considered the effect of FGR/FIR methods on decreasing of NO_x in swirl flame by using N_2 and CO_2 as diluent gases and observed that both gases are effective in reducing NO_x because of large temperature drop. Furthermore, several researchers studied the effect of diluent addition on flammability limits and emissions levels [10]-[12].

The objective of current computational research is mainly to investigate the effect of N_2 addition to the fuel stream on the flame structure and temperature distribution in a certain bluff-body stabilized methane swirling flame [13] with different swirl intensities.

II. The OpenFOAM Framework

OpenFOAM is an open source CFD software package written in C++, an object-oriented programming language. It contains numerous solvers which are designed to solve complex fluid flows involving combustion, turbulence and heat transfer. It also includes tools for meshing and utilities for post-processing and data manipulation. This package has been developed by OpenCFD Ltd at ESI Group and distributed by the OpenFOAM Foundation [14].

III. Combustion Model

In this research, the steady laminar flamelet model (SLFM) implemented in OpenFOAM has been used as combustion model. SLFM is based on the assumption that the turbulent flames can be considered as an ensemble of small laminar diffusion flames named as flamelets, in which the chemical reaction zone is thin enough compared to the turbulent length scales [16]. One of the most important advantages of the flamelet model is that the flamelets calculation is independent

Yasaman Tohidi is with the Department of Aerospace Engineering, Faculty of New Sciences and Technologies, University of Tehran, Tehran, Iran (e-mail: yas.tohidi@ut.ac.ir).

Shidvash Vakilipour is with the Department of Aerospace Engineering, Faculty of New Sciences and Technologies, University of Tehran, Tehran, Iran (phone: 989121326951, e-mail: vakilipour@ut.ac.ir).

Saeed Ebadi Tavallaee is with the Department of Electrical Engineering, Iran University of Science and Technology, Tehran, Iran (e-mail: saeedebadi@gmail.com).

Shahin Vakilipoor Takaloo is with the Department of Management, Islamic Azad University, Qeshm, Iran (e-mail: shahinvakilipoor@gmail.com).

Hossein Amiri is with the Atra Crown Energy (ACE Oil) Company, Tehran, Iran (e-mail: amiri.hossein1965@gmail.com).

Open Science Index, Mechanical and Mechatronics Engineering Vol:13, No:7, 2019 publications.waset.org/10010559/pdf

from turbulent flow in the pre-processing step. In pre-processing step, flamelets are stored in a flamelet library. After that, thermodynamic properties and species mass fractions can be extracted from these tables using parameters such as mixture fraction (Z), its variance (Z''), and scalar dissipation rate (χ), transported in the turbulent code. The conservation equations of species mass fraction and temperature in the mixture fraction space can be written as:

$$\rho\frac{\partial y_k}{\partial t}-\frac{1}{2}\rho\chi\frac{\partial^2 y_k}{\partial z^2}-\omega_k=0 \quad (1)$$

$$\rho\frac{\partial T}{\partial t}-\frac{1}{2}\rho\chi\left(\frac{\partial^2 T}{\partial z^2}+\frac{1}{c_p}\frac{\partial c_p}{\partial Z}\frac{\partial T}{\partial Z}\right)+\frac{1}{c_p}\sum_{k=1}^{n}h_k\omega_k=0 \quad (2)$$

where ρ is the thermodynamic density, Y_k is the chemical species mass fraction, T denotes the temperature, c_p and h_k are the specific isobaric heat capacity and the specific enthalpy of species k, respectively. The chemical species source term which is marked by ω_k can be calculated with the chemistry reaction mechanism. The scalar dissipation rate, χ, is regarded as an inverse diffusion time scale.

$$\chi=2D\left(\frac{\partial Z}{\partial y}\right)^2 \quad (3)$$

χ is the function of mixture fraction and can be parameterized by its value at stoichiometric mixture, χ_{st}. In the current study, the flamelets are computed via the open-source chemistry software Cantera in which the scalar dissipation rate is adjusted by changing mass flow at fuel and oxidizer inlets.

Then, the mean value for species mass fraction and temperature are calculated by using Favre Presumed Probability Density Function (PDF).

$$\widetilde{Y_k}=\int_0^\infty\int_0^1 Y_k(Z,\chi_{st})P(Z,\chi_{st})dZd\chi_{st} \quad (4)$$

$$\widetilde{T_k}=\int_0^\infty\int_0^1 T(Z,\chi_{st})P(Z,\chi_{st})dZd\chi_{st} \quad (5)$$

Two additional transport equations for the mean mixture fraction and its variance have to be solved.

$$\frac{\partial\bar{\rho}\tilde{Z}}{\partial t}+\frac{\partial\bar{\rho}\tilde{u}_i\tilde{Z}}{\partial x_i}=\frac{\partial}{\partial x_i}\left(\mu_{eff}\frac{\partial\tilde{Z}}{\partial x_i}\right) \quad (6)$$

$$\frac{\partial\bar{\rho}\,\partial\widetilde{Z''^2}}{\partial t}+\frac{\partial\bar{\rho}\tilde{u}_i\,\partial\widetilde{Z''^2}}{\partial x_i}=\frac{\partial}{\partial x_i}\left(\mu_{eff}\frac{\partial\widetilde{Z''^2}}{\partial x_i}\right)+2\mu_{eff}\left(\frac{\partial\tilde{Z}}{\partial x_i}\right)^2-\bar{\rho}\tilde{\chi} \quad (7)$$

Here, the effective viscosity is consisted of a laminar and a turbulent contribution ($\mu_{eff}=\mu+\mu_t$) in which the eddy viscosity (μ_t) can be calculated by using a turbulence model.

The mean scalar dissipation rate in the mixture fraction variance equation can be modeled as:

$$\tilde{\chi}=C_\chi\frac{\varepsilon}{k}\widetilde{Z''} \quad (8)$$

$C_\chi=2$. Also here, k and $\mathcal{E}$ are the turbulent kinetic energy and its dissipation respectively. In this study, the chemical reaction mechanism applied for the CH_4 combustion is GRI 2.11 with 49 species and 277 reactions [17].

IV. Modified K-Epsilon Turbulence Model

Among the several turbulence models which have been employed for simulation of the bluff-body swirl flames, the modified k-epsilon model (by changing the constant $C\varepsilon_1$ from 1.44 to 1.6) has been proposed to improve the prediction of flow field and compensate for excessive diffusion [18], [19].

V. Numerical Modeling

The experimental data obtained by Al-Abdeli and Masri [13] were used for validation purpose. The schematic of burner is depicted in Fig. 1. The swirl burner is located in wind tunnel with about 2% free stream turbulence and the area of 130 mm square.

The 60 mm-diameter swirling annulus which provides the flow of pure air encompasses the stream of a fuel jet and a ceramic bluff-body face. In other words, fuel and oxidizer are separated by a bluff-body which generates recirculation zones in the flow field [13]. The diameter of the fuel jet and the bluff-body face is 3.6 and D=50 mm respectively.

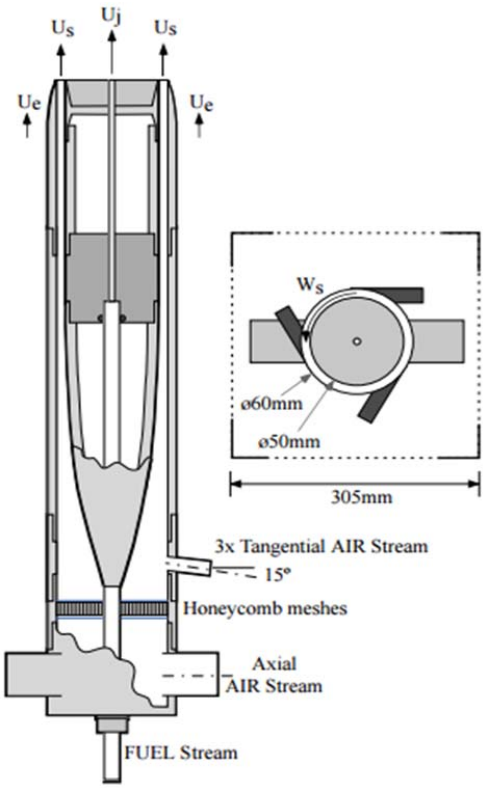


Fig. 1 The schematic of burner [20]

The boundary condition and flow properties of the reacting field such as the fuel jet velocity (U_j), the axial annular velocity (U_s), the tangential annular velocity (W_s) and the velocity of co-flow air stream in the wind tunnel (U_e) are listed in Table I.

In the current research the swirl number (S_g) sets to

W_s/U_s=0.5. Also, the Reynolds number of fuel jet and swirl air flow are considered to be 7200 and 75900 respectively.

A 2-D wedge-type computational domain which is discretized into 45000 cells (180 and 250 cells in radial and axial directions respectively) has been considered in this simulation. To obtain a better accuracy, a mesh structure with higher resolution close to the wall and inlet boundaries is defined.

TABLE I
FLOW PROPERTIES

case	Fuel	oxidizer	U_j (m/s)	U_s (m/s)	W_s (m/s)	U_e (m/s)
Swirl flame	Methane	air	32.7	38.2	19.1	20

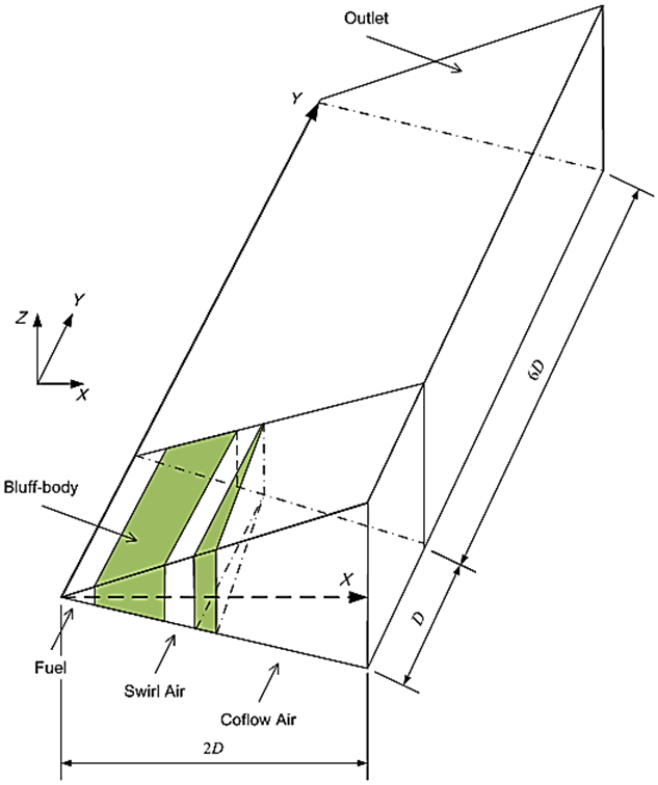


Fig. 2 The configuration of 2-D wedge-type computational domain

Fig. 2 shows the configuration of 2-D wedge-type grid. The flow field should be fully-developed at the exit plane. For this reason, the inlet flow streams are extended upstream of the exit plane to D=50 mm. In the current research, the OpenFOAM has been used as the computational toolbox. The code solves Favre-averaged Navier-Stokes and continuity equations. The Reynolds stresses are closed using modified *k*-epsilon model. The PISO algorithm is utilized for pressure-velocity coupling.

A Dirichlet condition is applied in the inlet for the velocity and mixture fraction fields and a Neumann condition is set in the outlet boundary. Also, the pressure is fixed in the outlet and side boundaries while a Neumann condition is applied for the inflow.

VI. Results and Discussion

A. Grid Dependency

The grid independency study has been done by changing the number of cells from 15000 to 75000 considering a mesh structure with higher resolution in the regions with high gradient of swirl velocity. This is because the most deviation from experimental data has been observed in the regions with higher velocity gradients. In Fig. 3, the effects of three different grids on the velocity and temperature profiles have been investigated in certain axial locations.

Although the grid with 15000 cells is unable to predict the aforementioned profiles properly, the difference between the simulation results of 45000 and 75000 cells is negligible, and no significant changes are observed in the simulation results. Consequently, the grid with 45000 cells has been utilized in this study.

B. Validation

Simulation results are compared with experimental data and previous studies [15] for axial velocity component and temperature. These results are depicted in Figs. 4 and 5. This comparison reveals that the predicted results are in a good agreement with the measurements and the general trend of profiles can be captured with an acceptable accuracy. It is worth to mention that a similar level of accuracy has already been reported regarding the simulation of this swirl flame in previous related studies [15]. Fig. 4 compares the calculated axial velocity component with measurements in different axial locations. It shows an over-prediction around the centerline at the axial location of y = 40 mm. This can be explained considering the low capability of RANS models regarding the simulation of shear flows.

C. Effect of N_2 Addition to the Fuel Stream

The objective of the present research is to numerically investigate the effects of N_2 addition to the fuel stream and study its effect on the structure and temperature distribution of swirl flames with different swirl intensity. To achieve this aim, different amount of N_2 is added to the fuel stream. The velocity boundary condition and the jet nozzle diameter kept unchanged and consequently, the mass flow rate of the fuel stream increases by addition of N_2.

There are different definitions for the non-premixed turbulent flame length (L). The first one is that it can be determined based on the visible flame length. The second definition is that the flame length would be the axial location of peak temperature on the centerline. Also, the third definition states that flame length is considered as axial distance in which the mixture fraction would be stoichiometric on the centerline.

Since the studied flame structure in the present research has an hourglass shape, the farthest stoichiometric mixture fraction point is not always on the centerline. In this regard, the flame length is defined as the largest vertical distance between the nozzle exit plane and the stoichiometric mixture fraction point [15].

Open Science Index, Mechanical and Mechatronics Engineering Vol:13, No:7, 2019 publications.waset.org/10010559/pdf

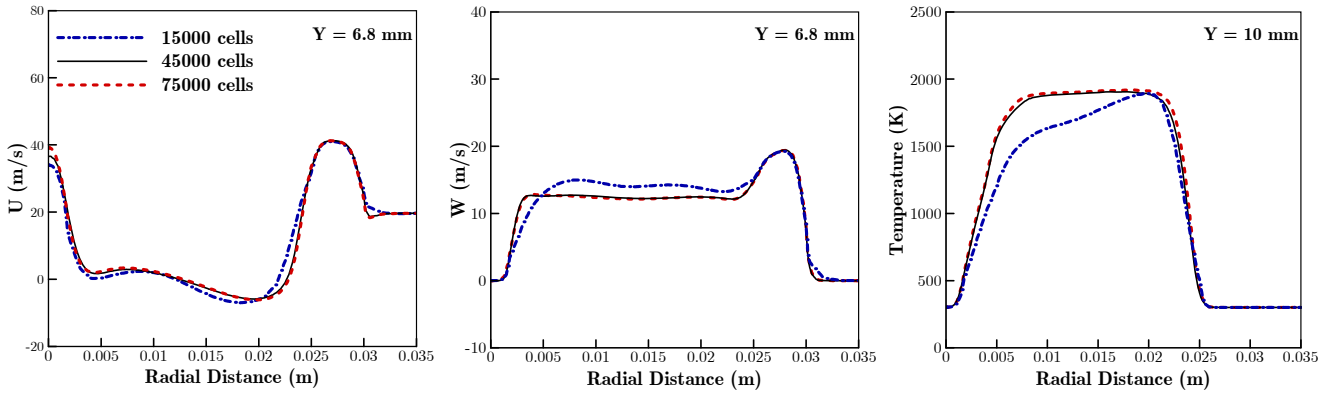


Fig. 3 Grid resolution study for radial profile of predicted temperature and velocity components at different axial locations using three mesh structure with 15000, 45000 and 75000 cells

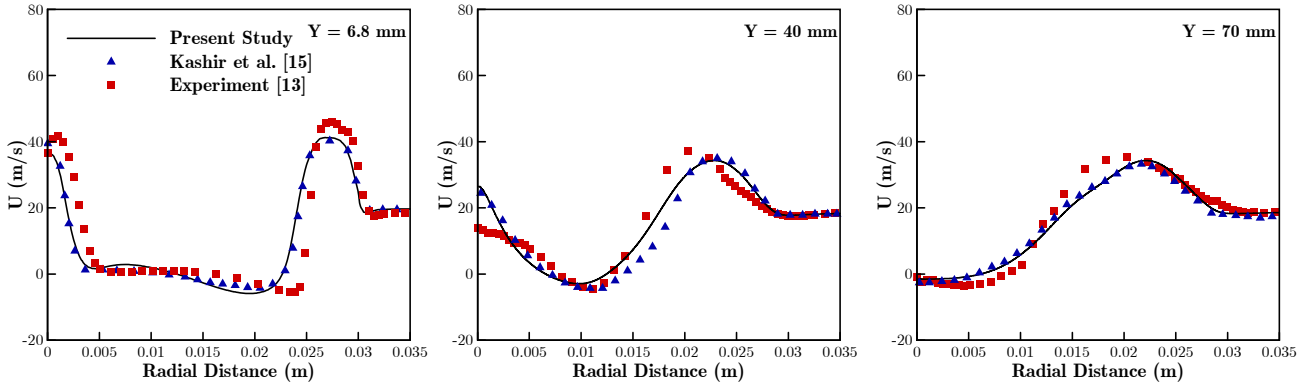


Fig. 4 Radial profile of predicted axial velocity component compared with measurements at different axial locations

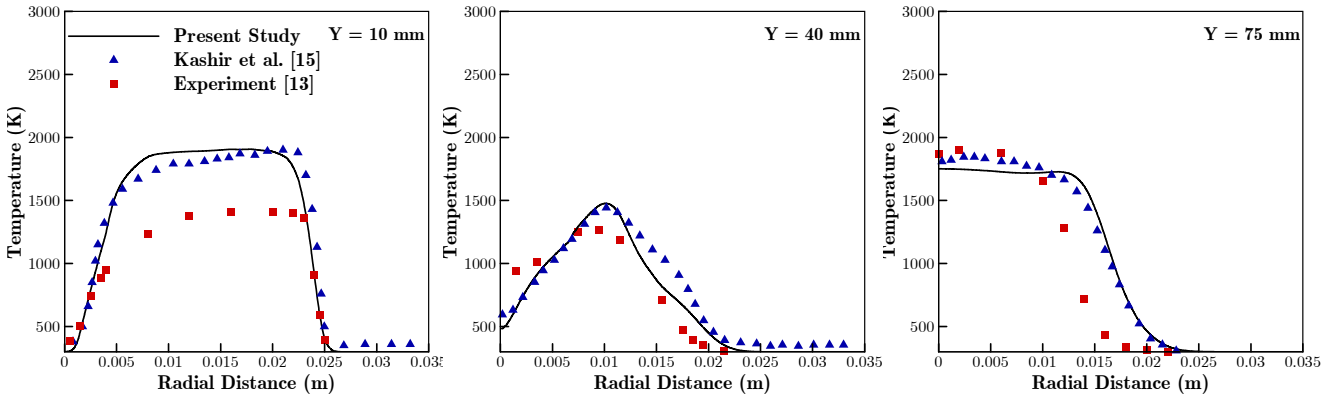


Fig. 5 Radial profile of predicted temperature compared with measurements at different axial locations

The details of different N_2 dilution cases are depicted in Table II. The flame length is decreased slightly with the addition of N_2. Actually, adding N_2 to the fuel stream decreases combustible components of fuel which leads to the reduction of mixing time and therefore decreases the flame length. On the other hand, this decrement is slight because N_2 dilution increases the mass flow rate of fuel jet which forces it to penetrate more in the downstream of the burner, however the effects of mixing are dominant and dilution effect decreases the flame length.

TABLE II
THE PERCENTAGE OF DILUTION AND CORRESPONDING DATA IN DIFFERENT CASES

Case	Fuel Composition	Z_{st}	S_g	L/D
Case 1	CH_4	0.055	0.5	2.06
Case 2	90%CH_4+10%N_2	0.065	0.5	1.98
Case 3	80%CH_4+20%N_2	0.077	0.5	1.93
Case 4	90%CH_4+10%N_2	0.065	0.3	2.82
Case 5	80%CH_4+20%N_2	0.077	0.3	2.61
Case 6	90%CH_4+10%N_2	0.065	0.6	1.79
Case 7	80%CH_4+20%N_2	0.077	0.6	1.73

Open Science Index, Mechanical and Mechatronics Engineering Vol:13, No:7, 2019 publications.waset.org/10010559/pdf

Open Science Index, Mechanical and Mechatronics Engineering Vol:13, No:7, 2019 publications.waset.org/10010559/pdf

Fig. 6 demonstrates the radial temperature profile at axial location of y = 100 mm in the case of N_2 addition to the fuel stream. This axial location is a critical region since it is located in the recirculation zone created by swirl effects.

It is observed that the increase of diluents molar concentration leads to the flame temperature reduction in this axial location. In the higher concentration of CH_4, the more breaking of exothermic bonds of carbon atoms in the hydrocarbon fuel leads to higher flame temperature. The lower amount of reactive species along with the high heat capacity of N_2 reduces the flame temperature.

The effect of N_2 addition to the fuel stream on the flame temperature distribution along the centerline is depicted in Fig. 8. This figure indicates that the temperature decreases by addition of N_2. It is worth to mention that compared with undiluted case, the peak temperature in Fig. 7 reduces around 14 and 35 K by adding the amount of 10% and 20% of N_2 respectively. It is also interesting that the maximum flame temperature on the centerline (which can be assumed as a measure of flame length) moves toward the upstream of the flow.

In the current study, a geometric swirl number S_g, which is the ratio of circumferential velocity to axial velocity is utilized to indicate the swirl intensity. Fig. 8 shows the structure of swirl flame in distinct dilution cases and different swirl intensities. In low swirl intensity (S_g = 0.3), the flame has a conical shape meaning that the maximum flame temperature is located on the centerline of the nozzle. On the other hand, the flame length has an hour-glass shape in high swirl intensities (S_g = 0.6) which means that the maximum flame temperature is located on the edges of the flame. The flame front is depicted in Fig. 9 by a black line. This line easily reveals the differences between the conical and hour-glass structure of flames. By increasing the swirl intensity, the flame length decreases significantly. This is because the increment of the oxidizer momentum leads to the production of stronger recirculation zones in the flow field which can increase the degree of mixing. This increment in mixing causes the reduction of flame length. As shown in Table II, the increasing of N_2 (compared to the undiluted case) leads to the decreasing of flame length in all swirl intensities; however, the rate of reduction is more significant in low swirl number.

VII. Conclusion

In the current research, the effect of N_2 addition to the fuel stream on the characteristics of swirl diffusion flames with distinct swirl intensities was numerically studied. In the validation section, the simulation results are compared with the measurements and the result reported by previous related studies. The comparisons showed that numerical results were able to capture the main trend of temperature and axial velocity component with an acceptable accuracy. In the next step, the effect of N_2 dilution was studied. Results depicted that the addition of N_2 to the fuel stream decreases the flame length and flame temperature. In high swirl intensity, the flame length is shorter compared to low swirl intensity case which is due to the higher level of mixing in S_g = 0.6. The flame length is reduced by addition of N_2 in all swirl numbers, but the rate of reduction is more significant in S_g = 0.3.

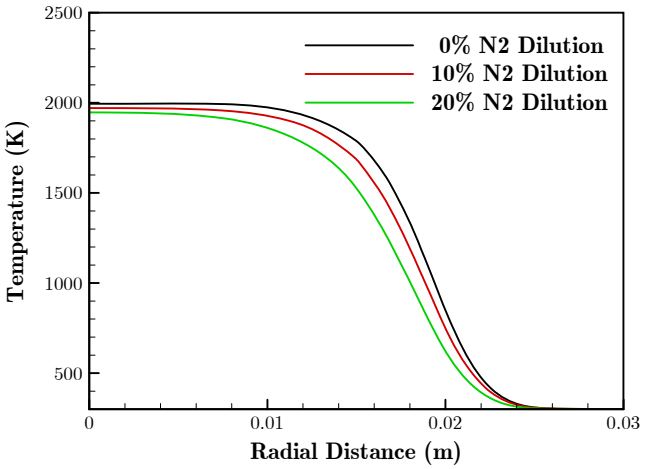


Fig. 6 Effect of N_2 dilution on the flame temperature distribution at axial location of y = 100 mm

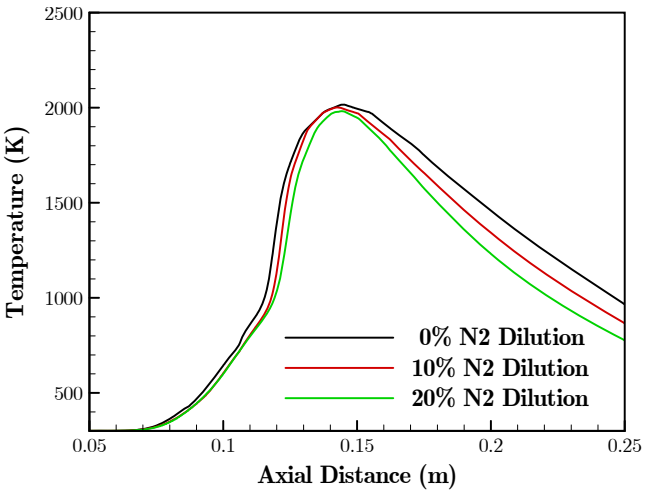


Fig. 7 Effect of N_2 dilution on the flame temperature distribution along the centerline of nozzle

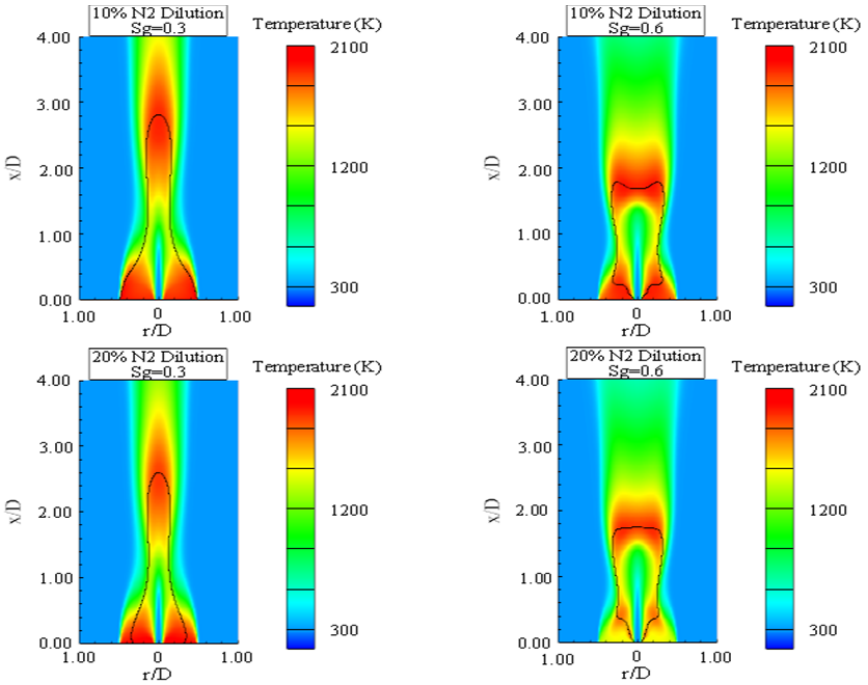


Fig. 8 The temperature contours in distinct dilution cases and different swirl intensities

REFERENCES

[1] Pope III CA, Ezzati M, Dockery DW. Fine-particulate air pollution and life expectancy in the United States. N Engl J Med. 2009 Jan 22;2009(360):376-86.

[2] Liu CY, Chen G, Sipöcz N, Assadi M, Bai XS. Characteristics of oxy-fuel combustion in gas turbines. Applied Energy. 2012 Jan 31;89(1):387-94.

[3] Zheng M, Reader GT, Hawley JG. Diesel engine exhaust gas recirculation—a review on advanced and novel concepts. Energy conversion and management. 2004 Apr 30;45(6):883-900.

[4] Park J, Kim SG, Lee KM, Kim TK. Chemical effect of diluents on flame structure and NO emission characteristic in methane-air counterflow diffusion flame. International Journal of Energy Research. 2002 Oct 25;26(13):1141-60.

[5] Zhuo L, Jiang Y, Qiu R, An J, Xu W. Effects of Fuel-Side N2, CO2, H2O Dilution on Combustion Characteristics and NOx Formation of Syngas Turbulent Nonpremixed Jet Flames. Journal of Engineering for Gas Turbines and Power. 2014 Jun 1;136(6):061505.

[6] Wang L, Liu Z, Chen S, Zheng C, Li J. Physical and chemical effects of CO2 and H2O additives on counterflow diffusion flame burning methane. Energy & fuels. 2013 Dec 9;27(12):7602-11.

[7] Xu H, Liu F, Sun S, Zhao Y, Meng S, Tang W. Effects of H 2 O and CO 2 diluted oxidizer on the structure and shape of laminar coflow syngas diffusion flames. Combustion and Flame. 2017 Mar 31;177:67-78.

[8] Gascoin N, Yang Q, Chetehouna K. Thermal effects of CO 2 on the NO x formation behavior in the CH 4 diffusion combustion system. Applied Thermal Engineering. 2017 Jan 5;110:144-9.

[9] Cho ES, Chung SH. Characteristics of NOx emission with flue gas dilution in air and fuel sides. KSME International journal. 2004 Dec 1;18(12):2303-9.

[10] Gu M, Chu H, Liu F. Effects of simultaneous hydrogen enrichment and carbon dioxide dilution of fuel on soot formation in an axisymmetric coflow laminar ethylene/air diffusion flame. Combustion and Flame. 2016 Apr 30;166:216-28.

[11] Yu B, Lee S, Lee CE. Study of NO x emission characteristics in CH 4/air non-premixed flames with exhaust gas recirculation. Energy. 2015 Nov 30;91:119-27.

[12] Roy RN, Sreedhara S. A numerical study on the influence of airstream dilution and jet velocity on NO emission characteristics of CH 4 and DME bluff-body flames. Fuel. 2015 Feb 15;142:73-80.

[13] Al-Abdeli YM, Masri AR. Stability characteristics and flow fields of turbulent non-premixed swirling flames. Combustion Theory and Modelling. 2003 Dec 1;7(4):731-66.

[14] URL http://www.openfoam.org. (No date).

[15] Kashir B, Tabejamaat S, Jalalatian N. A numerical study on combustion characteristics of blended methane-hydrogen bluff-body stabilized swirl diffusion flames. International Journal of Hydrogen Energy. 2015 May 18;40(18):6243-58.

[16] Peters N. Turbulent Combustion. Cambridge University Press; 2000.

[17] URL http://www.me.berkeley.edu/gri_mech/. (Accessed 3 November 1995).

[18] Dally BB, Fletcher DF, Masri AR. Flow and mixing fields of turbulent bluff-body jets and flames. Combustion Theory and Modelling. 1998 Jun 1;2(2):193-219.

[19] Sreedhara S, Huh KY. Modeling of turbulent, two-dimensional nonpremixed CH 4/H 2 flame over a bluffbody using first-and second-order elliptic conditional moment closures. Combustion and flame. 2005 Oct 31;143(1):119-34.

[20] Kalt PA, Al-Abdell YM, Masri AR, Barlow RS. Swirling turbulent non-premixed flames of methane: flow field and compositional structure. Proceedings of the Combustion Institute. 2002 Jan 1;29(2):1913-9.

Open Science Index, Mechanical and Mechatronics Engineering Vol:13, No:7, 2019 publications.waset.org/10010559/pdf